# Microstructural and transport properties of Mg doped CuFeO2 thin films: A promising material for high accuracy miniaturized temperature sensors based on the Seebeck effect

Inthuga Sinnarasa, Yohann Thimont, Antoine Barnabé, Mickael Beaudhuin, Adrien Moll, Juliano Schorne-Pinto, Philippe Tailhades, Lionel Presmanes

▶ **To cite this version:**

Inthuga Sinnarasa, Yohann Thimont, Antoine Barnabé, Mickael Beaudhuin, Adrien Moll, et al.. Microstructural and transport properties of Mg doped CuFeO2 thin films: A promising material for high accuracy miniaturized temperature sensors based on the Seebeck effect. Journal of Alloys and Compounds, 2020, 827, pp.154199. 10.1016/j.jallcom.2020.154199 . hal-02498344

**HAL Id: hal-02498344**

**https://hal.umontpellier.fr/hal-02498344v1**

Submitted on 11 Mar 2020

**HAL** is a multi-disciplinary open access archive for the deposit and dissemination of scientific research documents, whether they are published or not. The documents may come from teaching and research institutions in France or abroad, or from public or private research centers.

L'archive ouverte pluridisciplinaire **HAL**, est destinée au dépôt et à la diffusion de documents scientifiques de niveau recherche, publiés ou non, émanant des établissements d'enseignement et de recherche français ou étrangers, des laboratoires publics ou privés.

OATAO
Open Archive Toulouse Archive Ouverte

Open Archive Toulouse Archive Ouverte (OATAO)

OATAO is an open access repository that collects the work of Toulouse researchers and makes it freely available over the web where possible

This is an author's version published in: http://oatao.univ-toulouse.fr/25604

**Official URL:** https://doi.org/10.1016/j.jallcom.2020.154199

**To cite this version:**

Sinnarasa Barthelemy, Inthuga and Thimont, Yohann and Barnabé, Antoine and Beaudhuin, Mickael and Moll, Adrien and Schorne-Pinto, Juliano and Tailhades, Philippe and Presmanes, Lionel *Microstructural and transport properties of Mg doped CuFeO2 thin films: A promising material for high accuracy miniaturized temperature sensors based on the Seebeck effect.* (2020) Journal of Alloys and Compounds, 827. 154199. ISSN 0925-8388

Any correspondence concerning this service should be sent to the repository administrator: tech-oatao@listes-diff.inp-toulouse.fr

# Microstructural and transport properties of Mg doped $CuFeO_2$ thin films: A promising material for high accuracy miniaturized temperature sensors based on the Seebeck effect

Inthuga Sinnarasa [a], Yohann Thimont [a,*], Antoine Barnabé [a], Mickael Beaudhuin [b], Adrien Moll [b], Juliano Schorne-Pinto [a], Philippe Tailhades [a], Lionel Presmanes [a]

[a] CIRIMAT, Université de Toulouse, CNRS, INPT, Université Paul Sabatier, 118 route de Narbonne, 31062 Toulouse Cedex 9, France
[b] ICGM, Université de Montpellier, CNRS, ENSCM, Montpellier, France

ARTICLE INFO

*Keywords:*
Delafossite
Thin film
RF-Sputtering
Seebeck coefficient
Thin film thermal conductivity
Temperature sensors

ABSTRACT

Delafossite type Mg doped $CuFeO_2$ thin films have been deposited on fused silica by radio frequency magnetron sputtering. As deposited 300 nm thick films have been obtained and post annealed between 350 and 750 °C under primary vacuum. The delafossite structure appears for the samples annealed above 550 °C. The microstructural analysis showed the presence of cracks and an inhomogeneous distribution of the dopant in the thickness. Only the sample annealed at 700 °C showed $CuFeO_2$ stable phases, lower impurities amount, a high and constant Seebeck coefficient ($+416 \pm 3\ \mu V\ K^{-1}$) and good electrical conductivity ($1.08\ S\ cm^{-1}$ at 25 °C). High accuracy temperature sensors based on the Seebeck effect not only need high Seebeck coefficient without any drift with the temperature, but also a sufficient electrical conductivity and high phase stability. Thanks to its properties and also its low thermal conductivity ($4.8 \pm 0.6\ W\ m^{-1}K^{-1}$ at 25 °C) due to the thin film configuration and the polaronic transport, the Mg doped $CuFeO_2$ thin film annealed at 700 °C was found to be a very good p type material for high accuracy miniaturized temperature measurement sensors based on the Seebeck effect in the medium temperature range.

## 1. Introduction

$CuFeO_2$ is the first mineral to be called delafossite by the French chemist Charles Friedel [1]. This term is then generalized to an $AMX_2$ type structure. In such oxide family, i.e. when X is oxygen, the cation $A^I$ is a monovalent metal (Cu, Pt, Pd, Ag) and the cation $M^{III}$ is a trivalent metal (Al, Cr, Fe, Y, La, Sc, …). Delafossite structure can be described as a stack of cation $A^I$ layer and $MO_6$ octahedron layer along $\vec{c}$ axis. Each cation $A^I$ is linearly coordinated to two oxygens belonging to upper and lower $MO_6$. Delafossite compounds received much attention thanks to their good p type transparent conducting oxide properties [2], their unexpected magnetic [3] and conducting properties [4,5]. In the last decade, they showed also interesting thermoelectric properties due to their relatively high Seebeck coefficient [6–9].

$CuFeO_2$ is one of the delafossite oxides, which presents a polaronic conductivity. In particular, it arouses a great interest for its magnetic and magnetoelectric properties [10–13] but also for its optoelectronic [14–17] and thermoelectric [18–22] properties. These different properties have been improved thanks to doping (Ni [18], Mg [16], Pd [19],Pt [22], Co [23] and Ti [23]) and tuning oxygen stoichiometry [20,24]. The majority of studies on $CuFeO_2$ were conducted on bulk samples. $CuFeO_2$ has given rise to renewed interest in the recent years due to its photocatalytic properties for hydrogen production [17,25–27] as well as photovoltaic [28] properties.

Few authors have prepared this $CuFeO_2$ material in thin film form using different deposition techniques such as pulsed laser deposition [29–32], radio frequency sputtering [33,34], spin coating [35–37], electrodeposition [38] and spray pyrolysis [39]. In addition, the thermoelectric behavior of doped or undoped $CuFeO_2$ was rarely studied on thin films. Stocker et al. [24] are the only ones who have studied the thermoelectric properties of a $CuFeO_2$ thick film (25 μm thick) elaborated by an aerosol deposition.

Temperature sensors based on Seebeck effect firstly require high

* Corresponding author.
*E-mail address:* thimont@chimie.ups-tlse.fr (Y. Thimont).

https://doi.org/10.1016/j.jallcom.2020.154199

Seebeck coefficients and low Seebeck coefficient drift with the temperature. Conventional materials used in thermocouple as Chromel and Alumel show a relatively small Seebeck coefficient (<40 μV/K) and have a relatively high Seebeck coefficient drift with the temperature (as example, Chromel with 0.5% of Cr drift varies from 0 to 30 μV/K when the temperature increases from 0 °C to 1200 °C) [40]. This drift must be compensated by electronic setup which increase the global cost of the temperature sensors and can limit the measurement accuracy.

Temperature sensors based on Seebeck effect require also a low thermal conductivity and low material quantity to avoid thermal pumping. In previous work [41], we have demonstrated that in the case of thin films, the thermoelectric material can be considered as a composite made with the substrate and the thin film. The substrate does not participate to the electrical conduction and the Seebeck effect but it definitely influences the thermal conductivity. Besides, in the case of a lot of thin films, the thermal conductivities of the composite (film and substrate) can be assimilated to those of the substrate and could be advantageous for miniaturized temperature sensors when the substrates have small thermal conductivities.

Due to the specific needs for high accuracy miniaturized temperature sensors based on the Seebeck effect, in this article we have studied structural, microstructural and transport properties of Mg doped $CuFeO_2$ thin films deposited using RF magnetron sputtering to determine if their properties are adapted to high accuracy miniaturized temperature sensors application.

## 2. Experimental

### 2.1. Preparation of Mg doped $CuFeO_2$ target

Polycrystalline $CuFe_{0.97}Mg_{0.03}O_2$ (denoted $CuFeO_2$:Mg in the following) powder was prepared according to previous work [42,43] by grinding and mixing commercial oxides, $Cu_2O$, $Fe_2O_3$, and MgO with stoichiometric proportions. The oxide mixture was annealed at 900 °C for 10 h in nitrogen atmosphere and cooled down to room temperature. After it was ground again, the mixture was reheated for a further 10 h period. The purity of the delafossite phase was checked by X Ray Diffraction (XRD).

The polycrystalline delafossite powder has been pressed into a sputtering target of 10 cm in diameter then sintered at 1000 °C for 5 h in argon atmosphere.

### 2.2. Preparation of Mg doped $CuFeO_2$ thin films

In order to deposit $CuFeO_2$:Mg thin films, the target assembly was mounted in a RF magnetron sputtering chamber (Alcatel A450). The target was then initialized by sputtering its surface for 10 h. 15 min of pre sputtering with argon plasma has been applied before starting each film deposition to remove the surface contamination. Fused silica substrates (25 mm × 25 mm, ≃1 mm thick) placed on a water cooled sample holder were used during the deposition. In order to avoid the reduction of the target, a low argon pressure was used during the sputtering process [44]. The deposition parameters are summarized in Table 1. Under these conditions, as deposited films with thickness of 300 nm have been elaborated. The as deposited films have been systematically annealed for 4 h under primary vacuum at various temperatures between 350 and 750 °C.

**Table 1**
Process parameters for the deposition of delafossite Mg-doped $CuFeO_2$ by RF-sputtering.

| Target material | 3 $_{at\ \%}$ Mg-doped $CuFeO_2$ |
|---|---|
| Substrate | Fused silica |
| Power (W) | 50 |
| Magnetron | Yes |
| Argon pressure P (Pa) | 0.5 |
| Target to substrate distance d (cm) | 5 |

### 2.3. Characterization

Thickness measurements were performed with a DEKTAT 3030ST profilometer on a step made in the thin film. The composition of thin films has been checked using a CAMECA SXFiveFE Field Emission Gun Electron Probe Micro Analyser (FEG EPMA). The structural properties of the films were investigated by a α 1° Grazing Incidence X Ray Diffraction (GIXRD) at room temperature. GIXRD was performed using a Bruker D8 diffractometer equipped with a Bruker LynxEye 1D detector. Copper radiations were used as X ray source ($\lambda CuK_{\alpha 1}$ 1.5405 Å and $\lambda CuK_{\alpha 2}$ 1.5445 Å). The microstructure of the films was observed using a Jeol JSM7800F Field Emission Gun Scanning Electron Microscope (SEM FEG) and a Jeol JEM ARM200F Cold FEG corrected Transmission Electron Microscope (TEM). Glow Discharge Optical Emission Spectrometry (GD OES) measurements (Horiba GD profiler 2) was used to carried out fast compositional depth profiling from the nanometer range up to several hundreds of microns in depths. EPMA, SEM, TEM and GDOES were carried out at the Raimond Castaing Microcaracterisation Centre in Toulouse.

The electrical resistivity was measured at different temperatures using a four point probe measurement unit (Signatone). A home made measurement setup has been used for the Seebeck coefficient determination as a function of temperature. Two independent heaters fitted to the thin film geometry have been used to apply a thermal gradient along the thin film. Electrical contacts were done with a 25 μm diameter aluminium wire bonder (HYBOND Model 626). The ohmic type behaviour (linearity of current vs voltage curve) of the electrical contacts has been checked systematically for all samples with a source meter (Keithley 2450) after bonding step. During the experiment, the voltage was measured with a nanovoltmeter (Keithley 2182A). Two carbon spots (with an emissivity of 0.97) were deposited on the surface of the thin films by spraying carbon solution through a shadow mask to accurately measure the surface temperature with an infrared camera. The two carbon spots were located at the same isothermal position than the electrical contacts. The mean temperature ($T_{Mean}$) was considered as the average between the temperature of the hot side ($T_{Hot}$) and that of the cold side ($T_{Cold}$).

The Seebeck coefficient $S(T_{Mean})$ at a given mean temperature can be calculated with:

$$S(T_{mean}) \quad S_{ref} \quad \frac{\Delta V}{\Delta T} \tag{1}$$

Where ΔV, and ΔT are respectively electric potential and temperature difference ($T_{Hot}$ $T_{Cold}$) measured on the film. $S_{ref}$ is the Seebeck coefficient of aluminium wires which is negligible in comparison with high values of delafossite thin films. The accuracy of the experimental setup was checked by using a $Ca_3Co_4O_9$ sample already measured elsewhere with a commercial apparatus (ZEM 3). The results were similar with a standard deviation of 7%. The cross plane thermal conductivity was measured with a homemade apparatus at Institute Charles Gerhard Montpellier, similar to that of Beaudhuin et al. [45], using the 3ω method and discussed in detail by Cahill [46]. The setup up is made of an ultra low distortion function generator (Stanford Research Systems DS 360), a Vishay variable resistor (temperature coefficient resistance of 15 ppm/°C)

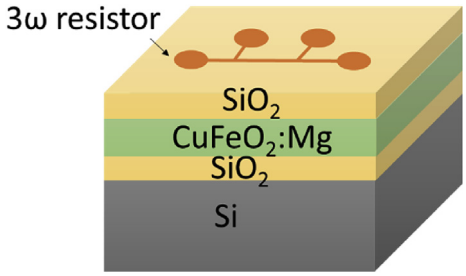


**Fig. 1.** Schematic representation of the sample used for the thermal conductivity measurement.

and an Analogical Digital Converter card model NI PCI 4474. To avoid the diffusion of Cu from delafossite into Si substrate, a 30 nm thick $SiO_2$ film was deposited beforehand on the substrate using chemical vapor deposition. The $CuFeO_2$:Mg thin film was electri cally isolated from 3ω resistor by depositing again a $SiO_2$ film as shown in Fig. 1. A gold metallic strip, 4 mm length, 29 μm width was used as a Resistance Temperature Detector. The 3ω signal is then detected with a numerical lock in amplifier and the Coefficient Temperature Resistance of the strip is determined in situ using a Keitlhey 2400 SourceMeter. The measurement circuit works with the differential method and the sample is located in a vacuum chamber at $2.10^{-5}$ mbar.

## 3. Results and discussions

### 3.1. Atomic composition

The as deposited thin films were analyzed with EPMA to check the composition. Ten measurements were used to determine an average atomic ratio given in the Table 2.

The results show an excess of copper with a molar ratio x Cu/(Fe + Cu) 0.56 smaller than x 0.49 which correspond to the stoichiometric Mg doped delafossite (x 0.96/(1 + 0.96)). In the Cu–Fe–O system, Wuttig et al. [26] and E.A. Trofimov [47] have already reported such copper non stoechiometry in undoped copper iron delafossite, but without any structural proof of the presence of the pure delafossite phase. Schorne Pinto et al. [48] have recently demonstrated that the delafossite structure can accept a copper excess up to 14% in air, i.e. up to x 0.53 before any precipitation of copper single oxide.

Fig. 2 shows the phase diagram of the Cu–Fe–O system calcu lated using Factsage software from the thermodynamic model published Shishin et al. [49] and by Schorne Pinto et al. [48] for an oxygen pressure $pO_2$ $10^{-5}$ atm which corresponds to the $pO_2$ measured in the furnace during the annealing in this work. Based on previous experimental tests done under air and argon atmo sphere, the copper solubility in the delafossite structure is extrap olated in this plot at x 0.47. One can note that this phase diagram is only effective for bulk and undoped material. In the case of Mg doped thin films, due to the Mg doping level, the high surface to volume ratio and the mechanical stress generally found in thin films, the stability domains could vary slightly from this plot. Nevertheless, whereas the copper excess is equal to x 0.56 in our

**Table 2**
Atomic ratio of different elements of the delafossite.

| | Expected value | Measured value |
|---|---|---|
| Mg/(Mg + Fe) | 0.03 | 0.04 ± 0.01 |
| Cu/(Cu + Fe) | 0.51 | 0.56 ± 0.01 |

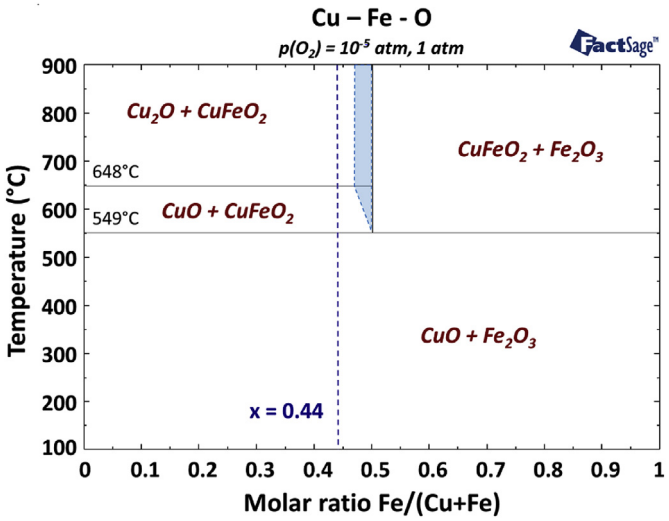


**Fig. 2.** Phase diagram of the Cu Fe O system calculated with Factsage software for an oxygen pressure of 8.6 Pa (pressure in the furnace) by using the data from Shishin et al. [49] and Pinto et al. [48] publications.

films, we can assume that a part of the copper could be inserted in the delafossite structure. If all the copper excess is not integrated into the delafossite structure, the rest of the copper should then form copper oxides like CuO or $Cu_2O$ below and above 648 °C respectively. The delafossite phase appears to be thermodynami cally stable above 549 °C.

### 3.2. Structural characterization

The GIXRD patterns of as deposited and annealed thin films between 350 and 750 °C are presented in the Fig. 3.

For T ≤ 500 °C, there were no diffraction peaks of delafossite structure. Only the diffraction peaks corresponding to the spinel and cuprite phases appeared gradually and increased in intensity until 500 °C. The diffraction peak at 2θ ≈ 35.8° was hardly assignable to a single phase because it could correspond to the most intense diffraction peaks of $CuFeO_2$ (012), CuO ( 111) and $CuFe_2O_4$ (311).

In the 500 < T ≤ 650 °C range, the peaks intensity corresponding to the spinel phase progressively decreased with the annealing

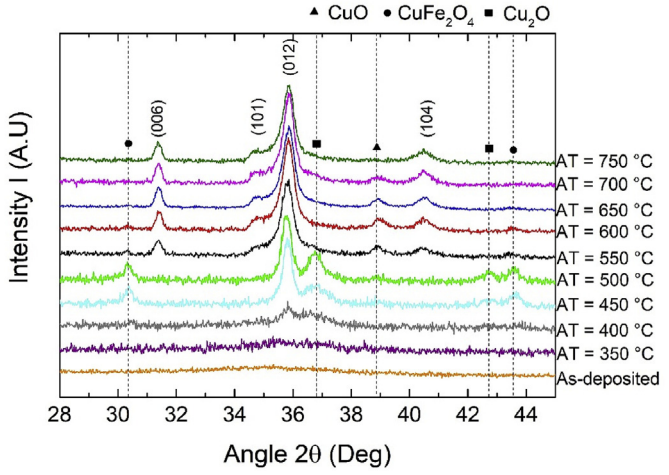


**Fig. 3.** GIXRD patterns of 300 nm thick $CuFeO_2$:Mg thin films annealed at various temperature under vacuum.

temperature, while the peaks corresponding to $CuFeO_2$ and CuO increased. Indeed, the most characteristic peaks of the delafossite structure indexed (006), (101), (012) and (104) in the trigonal R 3m space group (file: # 01 070 6670) were identifiable and their in tensity remained almost constant with the annealing temperature. The presence of $CuFeO_2$ and CuO phases well agrees with the calculated phase diagram (Fig. 2) in this temperature range.

For T > 650 °C, the characteristic peaks of cuprite decreased in intensity. Over 700 °C, no peak of the secondary phases can be observed, only the diffraction peaks of the $CuFeO_2$ phase were visible. The excess of Cu observed with EPMA was not visible on the GIXRD pattern for the films annealed at a temperature higher than 700 °C. This corroborate that all the coper excess could be inte grated into the delafossite structure. One can also note that no extra phase with Mg has been highlighted by GIXRD in all the temper ature range.

In addition, it is interesting to note on GIXRD pattern that the peak (006) of the $CuFeO_2$:Mg appears with an expected relative intensity for the delafossite structure, in contrary to the $CuCrO_2$:Mg thin films studied in our previous works [8,9] for which, there was an absence of crystallite oriented along the $\vec{c}$ axis. In $CuFeO_2$:Mg, no particular preferred orientation could be noticed.

The Raman spectra of the thin films annealed at 700 °C and 750 °C (Fig. 4) showed only the two Raman active modes $E_g$ and $A_{1g}$ at 349 $cm^{-1}$ and 688 $cm^{-1}$ respectively which was consistent with the spectra of the reference powder. The broad band around 500 $cm^{-1}$ was present both in the Raman spectra of the powder

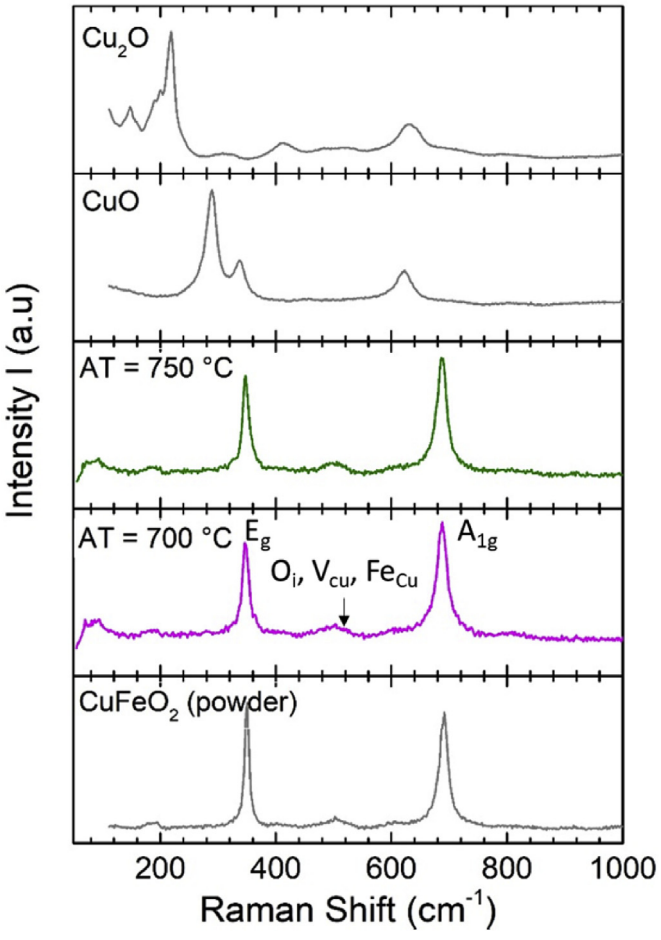


**Fig. 4.** Raman spectra 700 °C and 750 °C annealed thin films and the reference Raman spectra of $CuFeO_2$, CuO and $Cu_2O$.

that the thin films. It correspond to the relaxation of selection rules by defects such as interstitial oxygen's, Cu vacancies or tetrahe drally coordinated $Fe^{3+}$ on the Cu site [50]. The Raman active modes of CuO and $Cu_2O$ phases were not observable in the spectra of the thin films, proving once again the total solubility of copper excess into delafossite structure. Moreover, no vibration mode of MgO phase was detected which confirm the Mg insertion in the delafossite structure Therefore, based on the GIXRD and Raman analyses, the thin films annealed at 700 °C and 750 °C show a pure delafossite phase.

### 3.3. Microstructural characterization

Fig. 5 shows surface SEM FEG micrographs of 300 nm thick $CuFeO_2$:Mg thin films annealed at 600, 650, 700 and 750 °C. The SEM FEG micrographs show that for temperature higher than 650 °C, micro cracks appeared and increased in size and number. This could be a progressive relaxation by a cracking phenomenon due to an accumulation of tensile stress during the cooling steps when the sample has been annealed at T > 600 °C. It is explained by the large difference in the thermal expansion coefficient between $CuFeO_2$ ($30 \times 10^{-6}$ $K^{-1}$ estimated with the peaks shift of $CuFeO_2$ powder as a function of the temperature obtained with tempera ture dependent XRD not shown here) thin film and fused silica substrate ($0.5 \times 10^{-6}$ $K^{-1}$) [51,52].

A high resolution transmission electron microscopy study in dark and bright fields Scanning TEM modes (STEM) was used to characterize the thin film (Fig. 5). To avoid any mechanical artefact, a thin lamella was prepared by focused ion beam. Fig. 6 shows cross section STEM micrographs of $CuFeO_2$:Mg thin film annealed at 700 °C. The obtained micrographs showed the formation of voids at the interface between the thin film and the substrate. The cooling step following the annealing caused the differential withdrawal of the thin layer and the substrate according to their respective thermal expansion coefficients. This withdrawal ended up forming the cracks at the interface that amplified with temperature.

Fig. 7 shows the distribution of the chemical elements in the annealed thin film at 700 °C by Energy Dispersive X ray Spectros copy (EDS) mapping. Copper and iron were mostly homogeneously distributed except for few areas. The areas depleted of iron and rich in copper, which are perceptible on the EDS maps, can show the presence of $Cu_2O$ phases in agreement with the phase diagram (Fig. 2). Indeed, the quantitative analysis of this area showed that the atomic percentage of the copper is twice higher than that of oxygen. Besides, magnesium was not homogeneous throughout the film thickness. Its concentration was high at the surface and in some areas in the film close to the interface. This inhomogeneous distribution of chemical elements in the thin layer could signifi cantly affect its physical properties. However, according to Raman and GIXRD patterns of the thin film annealed at 700 °C, the ma jority of the crystalline phase was the delafossite $CuFeO_2$.

Fig. 8 exhibits the GDOES element profiles of $CuFeO_2$:Mg as deposited thin film and annealed thin film at 550 °C and 700 °C.

Fig. 8a) indicates that the as deposited thin film had a homo geneous distribution of the chemical elements in depth while the thin layer treated at 550 °C and 700 °C showed a progressive enrichment in magnesium at the surface and at the interface (Fig. 8b and c). Although in general, the interpretation of the results on the first sputtered layers is not significant, the observation of a high intensity for magnesium during the first seconds confirmed a high concentration on the surface in agreement with TEM study (Fig. 7c). The annealing process promoted the migration of mag nesium to the surface and the interface. Even if the GDOES and the TEM EDS analyses do not allow to probe the matter at the atomic scale, i.e. are not be able to quantify the degree of substitution of Fe

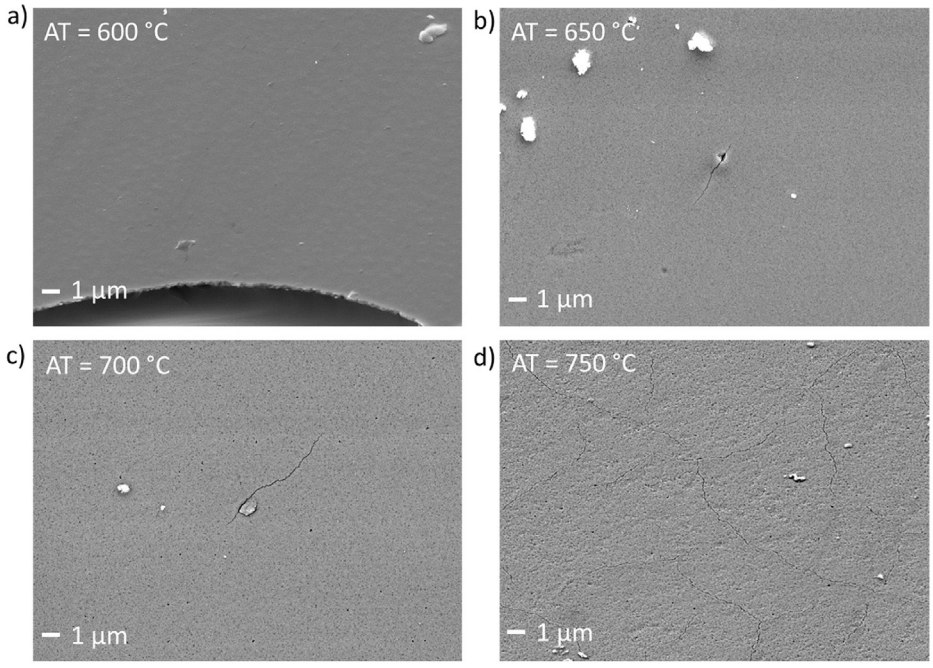


**Fig. 5.** Top surface SEM-FEG micrographs of 300 nm thick $CuFeO_2$:Mg thin films annealed at a) 600, b) 650, c) 700 and d) 750 °C.

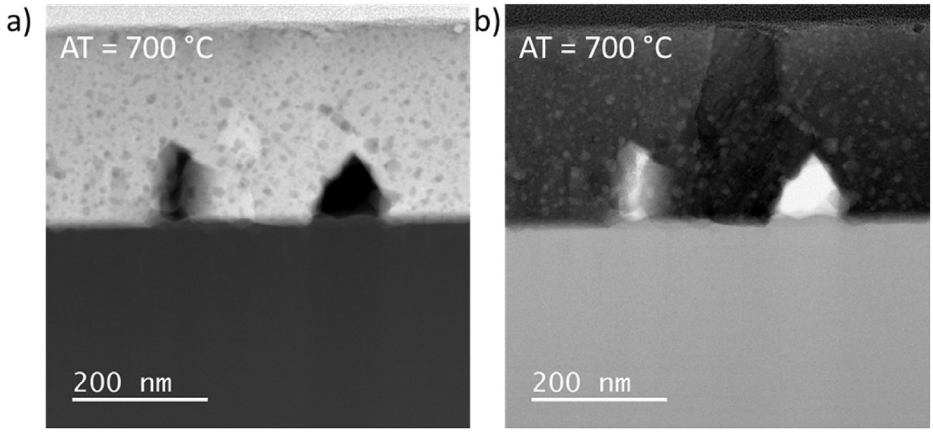


**Fig. 6.** a) Bright field and b) dark field cross section STEM micrographs of 300 nm thick $CuFeO_2$:Mg thin films annealed at 700 °C.

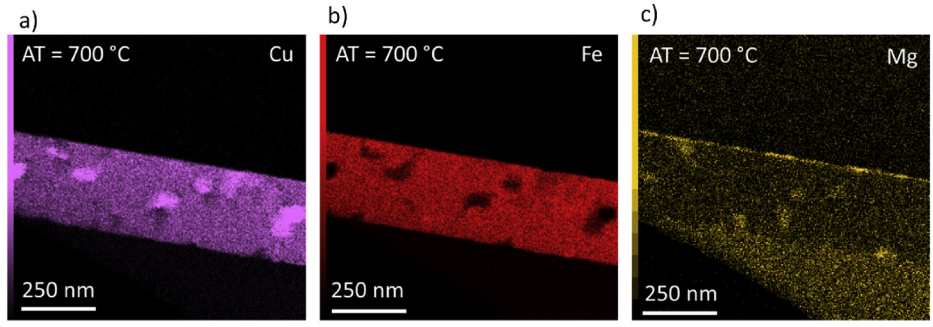


**Fig. 7.** Distribution of the chemical elements in the annealed thin film at 700 °C by EDS mapping of a) Cu, b) Fe and c) Mg.

by Mg within the delafossite structure, both results clearly indicate that the magnesium doping was not completely effective in the whole thickness of $CuFeO_2$:Mg thin films. Moreover, the Mg migration was getting stronger at the interfaces when the anneal ing temperature was increased.

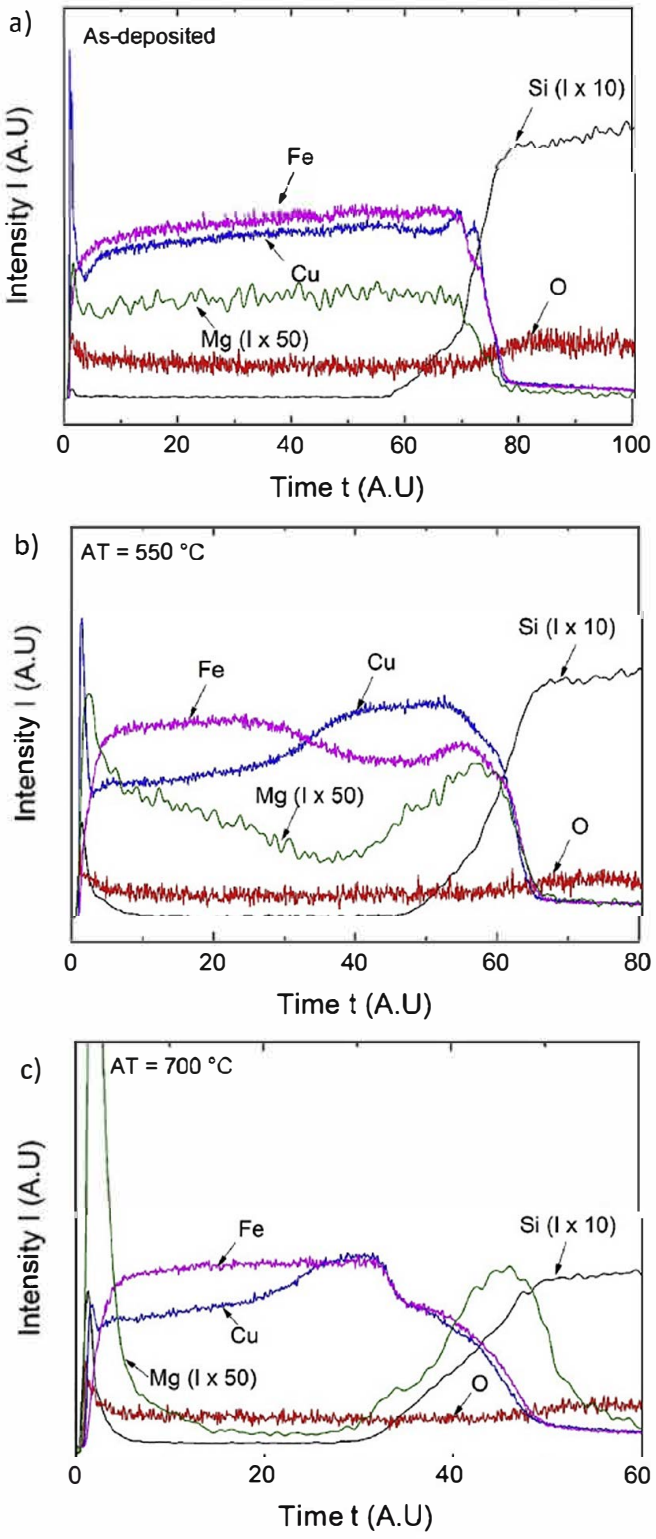


Fig. 8. Light emission spectrum given by GDOES of $CuFeO_2$:Mg a) as deposited thin film b) annealed at b) 550 °C and c) 700 °C.

## 4. Transport properties

### 4.1. Electrical conductivity

Unlike the Seebeck coefficient, a good electrical conductivity is not crucial for high accuracy temperature sensor application. Electrical conductivity must simply allow electrical measurements to be done. Only the thin films annealed above 550 °C which exhibit the delafossite phase have been studied in this part. Fig. 9 (top) shows the electrical conductivity at 25 °C of 300 nm thick films as a function of the measuring temperature. Semiconductor thermally polaronic transport identified by a linear regression of the ln ($\sigma$T) f(1000/T) plot was identified for each sample (in insert of the Fig. 9). In these cases, the electrical conductivity increases due to an increasing of the polaronic mobility. In the delafossite phase, the transport operates by hole polarons between $Cu^+$ and $Cu^{2+}$. $Fe^{3+}$ ions are substituted by $Mg^{2+}$ in the octeadron sites and leads to a copper mixed valence. The variation in electrical conductivity was similar during the increase and the decrease of the measuring

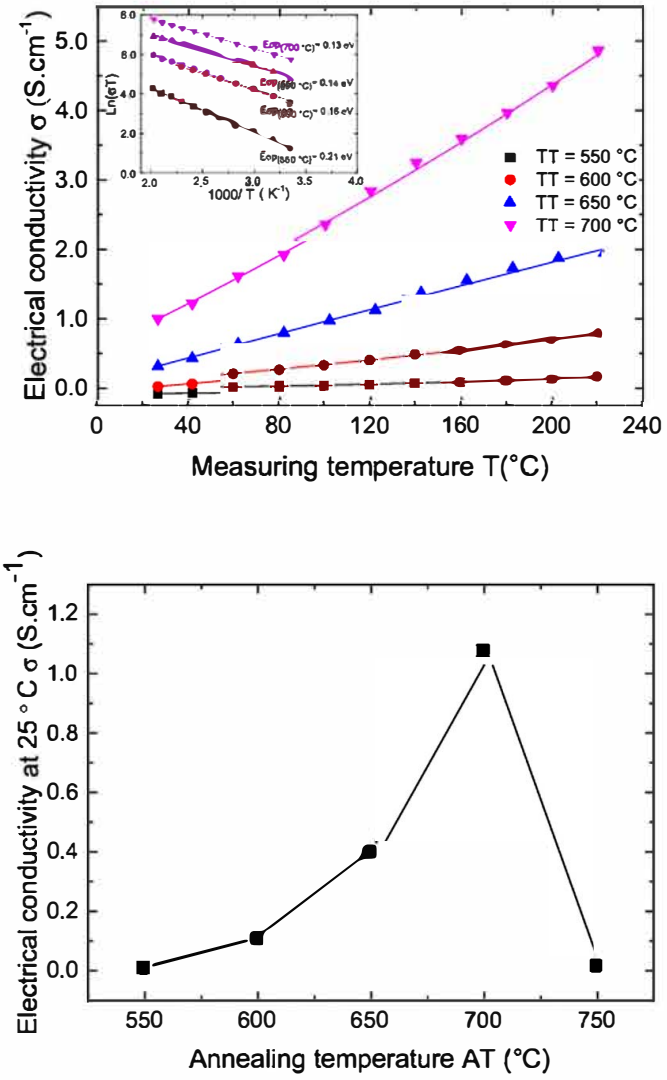


Fig. 9. (Top) Electrical conductivity as function of the measuring temperature of 300 nm thick $CuFeO_2$:Mg thin films annealed at various temperature. In insert ln($\sigma$T) as function of 1000/T for the 700 °C annealed $CuFeO_2$ thin film. (Bottom) Electrical conductivity at 25 °C of 300 nm thick $CuFeO_2$:Mg thin films as a function of the annealing temperature.

temperature. This confirms the stability of the $CuFeO_2$:Mg structure in the 25–250 °C temperature range in air. We can conclude that the structure and the Mg substitution in the delafossite structure are stable. The Fig. 9 (bottom) show that the electrical conductivity at room temperature increased with the annealing temperature up to 700 °C to reached 1.08 S $cm^{-1}$, then drastically decreased down to 0.02 S $cm^{-1}$ for the film annealed at 750 °C. The increase of the electrical conductivity can be explained by the effect of $CuFeO_2$ crystallization, the iron substitution by the magnesium and the purification of the $CuFeO_2$ delafossite phase in agreement with XRD data (Fig. 3) and the phase diagram (Fig. 2).

The stabilized $CuFeO_2$ phase (higher XRD peaks intensities) with lower copper oxide (CuO) impurity amount without thin film microcracks is only obtained after annealing treatment at 700 °C. Below this annealing temperature, the $CuFeO_2$ phase is not fully crystallized and the amount of impurity (in particular CuO which have low electrical conductivity ($<10^{-3}$ S $cm^{-1}$)) remains too high while over this annealing temperature, according to XRD, the phase is pure but microcracks appear (Fig. 5) leading to a drop of electrical conductivity.

The lowest polaronic transport activation energy is obtained for thin film annealed at 700 °C (when the $CuFeO_2$ is fully crystallized and the amount of impurity is low). The polaronic transport activation energy of the 700 °C annealed $CuFeO_2$ thin film is equal to 0.13 eV (Fig. 9 Insert).

The obtained electrical conductivity value (σ 1.08 S $cm^{-1}$ at 25 °C) for the annealed sample at 700 °C was higher than the value published by Deng et al. [15] (σ 0.31 S $cm^{-1}$ at room temperature) for 2% Mg doped $CuFeO_2$ thin film and by Chen et al. [14] (σ 0.36 S $cm^{-1}$ at room temperature) for the undoped $CuFeO_2$ thin film. However, Zhang et al. [35] found 1.72 S $cm^{-1}$ at room temperature for an epitaxial and undoped $CuFeO_2$ thin film where the absence of grain boundaries promoted electrical conduction.

### 4.2. Seebeck coefficient

High accuracy temperature sensor application needs high Seebeck coefficient without drift with the temperature. The Seebeck coefficient of $CuFeO_2$:Mg thin films annealed at various temperature is represented as a function of the measuring temperature in Fig. 10. The 750 °C annealed thin film has not been measured because of an insufficient electrical conductivity (due to the presence of microcracks).

The positive values of Seebeck coefficient of all thin films confirmed that the $CuFeO_2$:Mg thin films were a p type semiconductors. The Fig. 10 shows that the Seebeck coefficient decreases when the annealing temperature increase. It is coherent with the electrical conductivities which increase with the annealing temperature because it can be firstly explained by an increasing of the holes concentration due to a better substitution of the iron by the magnesium in the delafossite structure when annealing temperature increases. In a second hand, the copper oxide impurity plays a role on the Seebeck coefficient to contribute contribution to increasing this one. CuO is a p type band semiconductor therefore, its Seebeck coefficient decreases with the temperature. It can explain the observed drift of the Seebeck coefficient with the temperature for thin film annealed below 700 °C (those which have higher CuO amount). The values of the Seebeck coefficient of the 700 °C annealed thin film are systematically smaller than those of the other samples (+416 ± 3 μV $K^{-1}$) but remained constant with increasing temperature in agreement with a polaronic transport for which the carrier concentration remains constant with the temperature (only due to the Mg dopant).

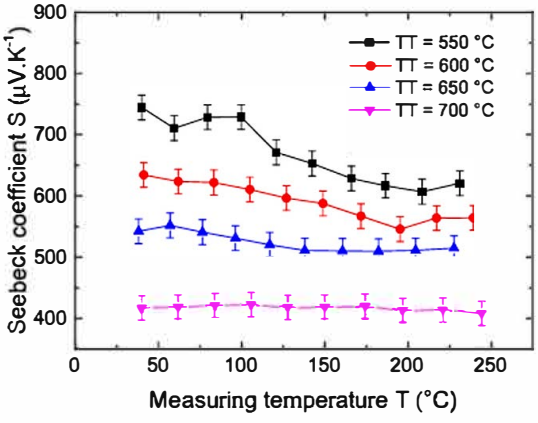


Fig. 10. Seebeck coefficient of 300 nm thick $CuFeO_2$:Mg thin films annealed at various temperatures as a function of the measuring temperature.

The drift of Seebeck coefficient with the temperature is not advantageous for high accurate temperature sensors. For this reason, the 700 °C annealed thin film is the only sample which showed the electronic transport properties required for high accurate temperature sensors. For this sample, the Seebeck coefficient was similar during the increase and the decrease of the measuring temperature which shows high stability.

Therefore, the hopping conduction could be attributed to this material where the density of charge carrier did not vary with temperature. Applying similar approach than those used for Mg doped $CuCrO_2$ [9], the hole density [$Cu^{2+}$] is equal to $3.40 \pm 0.15 \times 10^{19}$ $cm^{-3}$ in the case of the Mg doped $CuFeO_2$ thin film annealed at 700 °C. The hole density is about three time smaller than those of Mg doped $CuCrO_2$ thin films and could be explained by a lower Mg substitution in the lattice in agreement with the EDS map and GDOES which have showed Mg segregation close to the interfaces. The limit of Mg substitution is clearly smaller in the case of $CuFeO_2$ than the $CuCrO_2$ compound leading to a higher Seebeck coefficient for Mg doped $CuFeO_2$ which is advantageous for high accurate temperature sensors. Stocker et al. [24] have also reported a constant Seebeck coefficient of +425 μV $K^{-1}$ for an aerosol deposited $CuFeO_2$ films. However, the values of the Seebeck coefficient of $CuFeO_2$:Mg bulk reported in the literature are scattered. Benko and Koffyberg [16] published +359 μV $K^{-1}$ for 2% Mg doped $CuFeO_2$ and Nozaki et al.[23] reported an increasing Seebeck coefficient with the temperature for the same material.

### 4.3. Thermal conductivity

A low thermal conductivity of the material and a low material quantity are two factors which reduce the heat pumping by the temperature sensor leading to an increasing of the accuracy of the temperature surface measurement. The thermal conductivity of the 300 nm thick $CuFeO_2$:Mg film annealed at 700 °C as a function of the measuring temperature is presented in Fig. 11. We can suppose there are no thermal conductivity anisotropy because there are no specific crystallites preferred orientation and the microstructure do not show a typical columnar grains growth but a dense small grains. The low thermal conductivity obtained for this material (<5 W $m^{-1}$ $K^{-1}$ in the 25 < T < 70 °C temperature range) in contrary to other oxides such as single crystal bulk ZnO [53] (50W.$m^{-1}$.$K^{-1}$) is firstly explained by the microstructure of the film (small grains size) and could be also explained partially by the polaron conduction mechanism whereas the contribution of the carriers to the thermal conductivity was low. Moreover, the complex delafossite structure especially the $FeO_6$ octahedral stacks limits also the

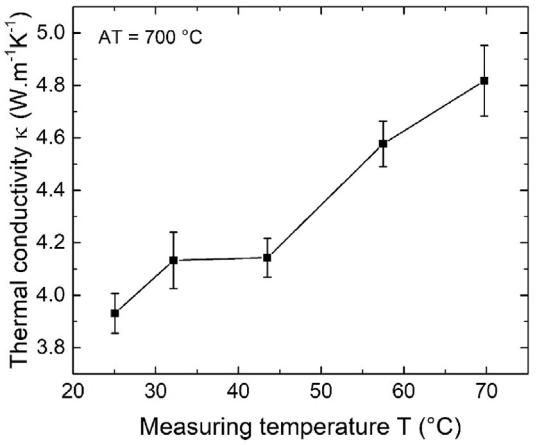


**Fig. 11.** Thermal conductivity of 300 nm thick $CuFeO_2$:Mg film annealed at 700 °C as a function of the measuring temperature.

phonon propagation. The obtained values of the thermal conductivity were lower than the values published by Nozaki et al. [54] (8.6 $Wm^{-1}K^{-1}$ at 28 °C) and by Ruttanapun et al. [55] (6.0 $Wm^{-1}K^{-1}$ at 31 °C) for $CuFeO_2$ bulk. The low value of thermal conductivity obtained in $CuFeO_2$:Mg thin film is in agreement with the normal behavior of thin film material. It can be explained by the effects of micro and nano structuration which cause a decrease of the thermal conductivity compared to the same bulk materials. Moreover, as described by Sinnarasa et *al* [41], the impact of thermal conductivity of the film can be neglected in comparison with the thermal conductivity of the substrate. In our case, the fused silica has a very low thermal conductivity (1.38 W $m^{-1}$ $K^{-1}$ at 300K) [56]. We can see that the thermal conductivity of $CuFeO_2$ material in thin film configuration is well adapted for high accuracy miniaturized temperature sensors.

## 5. Conclusions

300 nm thick $CuFeO_2$:Mg films have been deposited by RF magnetron sputtering and annealed between 350 and 750 °C under primary vacuum. The structural characterizations showed that for the films annealed above 550 °C, the main phase was delafossite. The microstructural characterizations revealed that cracks appeared on the films annealed above 650 °C and increased in number and size for samples annealed at higher temperature leading to a drastically decreasing of the electrical conductivity. Moreover, the dopant distribution was not homogenous in the films thickness which suggested that doping in $CuFeO_2$:Mg thin films was not completely effective. The best structural and microstructural properties were obtained for thin film annealed at 700 °C under primary vacuum. An electrical conductivity of 1.08 S $cm^{-1}$ at 25 °C and a high Seebeck coefficient ($+416 \pm 3$ μV $K^{-1}$) without drift with the temperature was obtained for this film. Moreover, the thermal conductivity of this thin film showed a low values (below 5W.$m^{-1}$.$K^{-1}$) in comparison with the bulk, allowing to reduce heat pumping and then to increase the accuracy of the temperature measurement. In the case of the optimized Mg doped $CuFeO_2$ thin film (annealed at 700 °C) all of properties are very well adapted to the p type part of high accuracy miniaturized temperature sensors based on the Seebeck effect in a medium temperature range. We can conclude that this material is a very good candidate for this kind of application.

## Declaration of competing interest

Authors declare no conflict of interest about the research and results reported in the submitted article.

## Acknowledgements

The authors would like to thank the French ministry of Research for the PhD funding.

## References

[1] C. Friedel, C.R. Hebd, Sur une combinaison naturelle des oxydes de fer et de cuivre, et sur la reproduction de l'atacamite, Seances Acad. Sci. 77 (1873) 211.
[2] H. Kawazoe, M. Yasukawa, H. Hyodo, M. Kurita, H. Yanagi, H. Hosono, P-type electrical conduction in transparent thin films of $CuAlO_2$, Nature 389 (1997) 939 942.
[3] T. Elkhouni, M. Amami, P. Strobel, A. Ben Salah, Structural and magnetic properties of substituted delafossite-type oxides $CuCr_{1-x}Sc_xO_2$, World J. Condens. Matter Phys. (2013) 1 8, 03.
[4] M. Ahmadi, M. Asemi, M. Ghanaatshoar, Improving the electrical and optical properties of $CuCrO_2$ thin film deposited by reactive RF magnetron sputtering in controlled $N_2$/Ar atmosphere, Appl. Phys. A 124 (2018) 529.
[5] D.O. Scanlon, A. Walsh, G.W. Watson, Understanding the p-type conduction properties of the transparent conducting oxide $CuBO_2$: a density functional theory analysis, Chem. Mater. 21 (2009) 4568 4576.
[6] E. Guilmeau, A. Maignan, C. Martin, Thermoelectric oxides: effect of doping in delafossites and zinc oxide, J. Electron. Mater. 38 (2009) 1104 1107.
[7] S. Saini, P. Mele, S. Osugi, M.I. Adam, Effect of oxygen pressure on thermoelectric properties of p-type $CuAlO_2$ films fabricated by pulsed laser deposition, J. Mater. Eng. Perform. 27 (2018) 6286 6290.
[8] I. Sinnarasa, Y. Thimont, L. Presmanes, C. Bonningue, A. Barnabé, P. Tailhades, Influence of thickness and microstructure on thermoelectric properties of Mg-doped $CuCrO_2$ delafossite thin films deposited by RF-magnetron sputtering, Appl. Surf. Sci. 455 (2018) 244 250.
[9] I. Sinnarasa, Y. Thimont, L. Presmanes, A. Barnabé, P. Tailhades, Thermoelectric and transport properties of delafossite $CuCrO_2$:Mg thin films prepared by RF magnetron sputtering, Nanomaterials 7 (2017) 157.
[10] K. Hayashi, R. Fukatsu, T. Nozaki, Y. Miyazaki, T. Kajitani, Structural, magnetic, and ferroelectric properties of $CuFe_{1-x}Mn_xO_2$, Phys. Rev. B 87 (2013), 064418.
[11] J.T. Haraldsen, F. Ye, R.S. Fishman, J.A. Fernandez-Baca, Y. Yamaguchi, K. Kimura, T. Kimura, Multiferroic phase of doped delafossite $CuFeO_2$ identified using inelastic neutron scattering, Phys. Rev. B 82 (2010), 020404.
[12] K. Hayashi, T. Nozaki, R. Fukatsu, Y. Miyazaki, T. Kajitani, Spin dynamics of triangular lattice antiferromagnet CuFeO2 : crossover from spin-liquid to paramagnetic phase, Phys. Rev. B 80 (2009) 144413.
[13] J.T. Haraldsen, R.S. Fishman, G. Brown, Spin-wave dynamics for the high-magnetic-field phases of the frustrated $CuFeO_2$ antiferromagnet: predictions for inelastic neutron scattering, Phys. Rev. B 86 (2012), 024412.
[14] H.-Y. Chen, J.-H. Wu, Transparent conductive $CuFeO_2$ thin films prepared by sol gel processing, Appl. Surf. Sci. 258 (2012) 4844 4847.
[15] Z. Deng, X. Fang, S. Wu, Y. Zhao, W. Dong, J. Shao, S. Wang, Structure and optoelectronic properties of Mg-doped $CuFeO_2$ thin films prepared by sol gel method, J. Alloys Compd. 577 (2013) 658 662.
[16] F.A. Benko, F.P. Koffyberg, Opto-electronic properties of p- and n-type delafossite $CuFeO_2$, J. Phys. Chem. Solid. 48 (1987) 431 434.
[17] Y. Oh, W. Yang, J. Tan, H. Lee, J. Park, J. Moon, Photoelectrodes based on 2D opals assembled from Cu-delafossite double-shelled microspheres for an enhanced photoelectrochemical response, Nanoscale 10 (2018) 3720 3729.
[18] T. Nozaki, K. Hayashi, T. Kajitani, Electronic structure and thermoelectric properties of the delafossite-type oxides $CuFe_{1-x}Ni_xO_2$, J. Electron. Mater. 38 (2009) 1282 1286.
[19] C. Ruttanapun, Effects of Pd substitution on the thermoelectric and electronic properties of delafossite $Cu_{1-x}Pd_xFeO_2$ (x 0.01, 0.03 and 0.05), J. Solid State Chem. 215 (2014) 43 49.
[20] C. Rudradawong, C. Ruttanapun, Effect of excess oxygen for $CuFeO_{2.06}$ delafossite on thermoelectric and optical properties, Phys. B Condens. Matter 526 (2017) 21 27.
[21] C. Ruttanapun, P. Jindajitawat, W. Thowladda, W. Neeyakorn, C. Thanachayanont, A. Charoenphakdee, Thermoelectric properties of $Sn^{2+}$-substituted $CuFeO_2$ delafossite-oxide, Adv. Mater. Res. 802 (2013) 17 21.
[22] C. Ruttanapun, A. Wichainchai, W. Prachamon, A. Yangthaisong, A. Charoenphakdee, T. Seetawan, Thermoelectric properties of $Cu_{1-x}Pt_xFeO_2$ ($0.0 \leq x \leq 0.05$) delafossite-type transition oxide, J. Alloys Compd. 509 (2011) 4588 4594.
[23] T. Nozaki, K. Hayashi, T. Kajitani, High temperature thermoelectric properties of delafossite-type oxides $CuFe_{0.98}M_{0.02}O_2$ (M Mg, Zn, Ni, Co, Mn, or Ti), in: I.C. Thermoelectrics (Ed.), 26th International Conference on Thermoelectrics, vol. 2, IEEE, 2007, pp. 167 170.
[24] T. Stocker, J. Exner, M. Schubert, M. Streibl, R. Moos, Influence of oxygen

partial pressure during processing on the thermoelectric properties of aerosol-deposited $CuFeO_2$, Materials 9 (2016) 227.
[25] Y.J. Jang, Y.B. Park, H.E. Kim, Y.H. Choi, S.H. Choi, J.-.S. Lee, Oxygen-intercalated $CuFeO_2$ photocathode fabricated by hybrid microwave annealing for efficient solar hydrogen production, Chem. Mater. 28 (2016) 6054 6061.
[26] A. Wuttig, J.W. Krizan, J. Gu, J.J. Frick, R.J. Cava, A.B. Bocarsly, The effect of Mg-doping and Cu nonstoichiometry on the photoelectrochemical response of $CuFeO_2$, J. Mater. Chem. 5 (2017) 165 171.
[27] M.S. Prévot, X.A. Jeanbourquin, W.S. Bourée, F. Abdi, D. Friedrich, R. Van de Krol, N. Guijarro, F. Le Formal, K. Sivula, Evaluating charge carrier transport and surface states in $CuFeO_2$ photocathodes, Chem. Mater. 29 (2017) 4952 4962.
[28] T. Crespo, Potentiality of $CuFeO_2$ -delafossite as a solar energy converter, Sol. Energy 163 (2018) 162 166.
[29] D.H. Choi, S.J. Moon, J.S. Hong, S.Y. An, I.-B. Shim, C.S. Kim, Impurity dependent semiconductor type of epitaxial CuFeO2 (111) thin films deposited by using a pulsed laser deposition, Thin Solid Films 517 (2009) 3987 3989.
[30] S.Z. Li, J. Liu, X.Z. Wang, B.W. Yan, H. Li, J.M. Liu, Epitaxial growth of delafossite $CuFeO_2$ thin films by pulse laser deposition, Phys. B Condens. Matter 407 (2012) 2412 2415.
[31] T. Joshi, T.R. Senty, R. Trappen, J. Zhou, S. Chen, P. Ferrari, P. Borisov, X. Song, M.B. Holcomb, A.D. Bristow, A.L. Cabrera, D. Lederman, Structural and magnetic properties of epitaxial delafossite $CuFeO_2$ thin films grown by pulsed laser deposition, J. Appl. Phys. 117 (2015), 013908.
[32] R.A. Wheatley, S. Rojas, C. Oppolzer, T. Joshi, P. Borisov, D. Lederman, A.L. Cabrera, Comparative study of the structural and optical properties of epitaxial $CuFeO_2$ and $CuFe_{1-x}Ga_xO_2$ delafossite thin films grown by pulsed laser deposition methods, *Thin Solid Films* 626 (2017) 110 116.
[33] A. Barnabé, E. Mugnier, L. Presmanes, P. Tailhades, Preparation of delafossite $CuFeO_2$ thin films by rf-sputtering on conventional glass substrate, Mater. Lett. 60 (2006) 3468 3470.
[34] E. Mugnier, A. Barnabé, L. Presmanes, P. Tailhades, Thin films preparation by rf-sputtering of copper/iron ceramic targets with Cu/Fe 1: from nano-composites to delafossite compounds, Thin Solid Films 516 (2008) 1453 1456.
[35] Li Zhang, P. Li, K. Huang, Z. Tang, G. Liu, Y. Li, Chemical solution deposition and transport properties of epitaxial $CuFeO_2$ thin films, *Mater. Lett.* 65 (2011) 3289 3291.
[36] H.Y. Chen, J.R. Fu, Delafossite $CuFeO_2$ thin films prepared by atmospheric pressure plasma annealing, Mater. Lett. 120 (2014) 47 49.
[37] A. Bera, K. Deb, S. Sinthika, R. Thapa, B. Saha, Chemical modulation of valance band in delafossite structured $CuFeO_2$ thin film and its photoresponse, Mater. Res. Express 5 (2018), 015909.
[38] C.G. Read, Y. Park, K.S. Choi, Electrochemical synthesis of p-type $CuFeO_2$ electrodes for use in a photoelectrochemical cell, J. Phys. Chem. Lett. 3 (2012) 1872 1876.
[39] A.H. Omran Alkhayatt, S.M. Thahab, I.A. Zgair, Structure, surface morphology and optical properties of post-annealed delafossite $CuFeO_2$ thin films, Opt. - Int. J. Light Electron Opt. 127 (2016) 3745 3749.
[40] M.V. Vedernikov, N.V. Kolomoets, Thermoelectric properties of solid solutions of chromium, vanadium and titanium in nickel, Sov. Phys. Solid State 2 (1961) 2420.
[41] I. Sinnarasa, Y. Thimont, L. Presmanes, A. Barnabé, P. Tailhades, Determination of modified figure of merit validity for thermoelectric thin films with heat transfer model: case of $CuCrO_2$ :Mg deposited on fused silica, J. Appl. Phys. 124 (2018) 165306.
[42] E. Mugnier, A. Barnabe, P. Tailhades, Synthesis and characterization of $CuFeO_{2+\delta}$ delafossite powders, Solid State Ionics 177 (2006) 607 612.
[43] M. Lalanne, A. Barnabé, F. Mathieu, P. Tailhades, Synthesis and thermo-structural studies of a $CuFe_{1-x}Cr_xO_2$ delafossite solid solution with $0 \leq x \leq 1$, Inorg. Chem. 48 (2009) 6065 6071.
[44] H. Le Trong, T.M.A. Bui, L. Presmanes, A. Barnabé, I. Pasquet, C. Bonningue, P. Tailhades, Preparation of iron cobaltite thin films by RF magnetron sputtering, Thin Solid Films 589 (2015) 292 297.
[45] M. Beaudhuin, L Van der Tampel, Thermal Conductivity Measurement of Thin Layers by the 3ω Method Philips Research TN-2006/**00375**.
[46] D.G. Cahill, Thermal conductivity measurement from 30 to 750 K: the 3ω method, Rev. Sci. Instrum. 61 (1990) 802 808.
[47] E. Trofimov, Thermodynamic Analysis of Phase Equilibrium in Multicomponent Systems Including Metallic Melts, *Metal* 2014, Brno, Czech Republic, EU.
[48] J. Schorne-Pinto, L. Cassayre, L. Presmanes, A. Barnabé, Insights on the stability and cationic nonstoichiometry of $CuFeO_2$ delafossite, Inorg. Chem. 58 (2019) 6431 6444.
[49] D. Shishin, T. Hidayat, E. Jak, S.A. Decterov, Critical assessment and thermodynamic modeling of the Cu Fe O system, Calphad 41 (2013) 160 179.
[50] O. Aktas, K.D. Truong, T. Otani, G. Balakrishnan, M.J. Clouter, T. Kimura, G. Quirion, Raman scattering study of delafossite magnetoelectric multiferroic compounds: $CuFeO_2$ and $CuCrO_2$, J. Phys. Condens. Matter 24 (2012), 036003.
[51] Key Geoffrey Lyon, Thermal expansion of glasses at low temperatures, Retrosp. Theses Diss. (1978) 6571.
[52] Z. Xia, J.W. Hutchinson, Crack patterns in thin films, J. Mech. Phys. Solid. 48 (2000) 1107 1131.
[53] X. Wu, J. Lee, V. Varshney, J.L. Wohlwend, A.K. Roy, T. Luo, Thermal conductivity of wurtzite zinc-oxide from first-principles lattice dynamics a comparative study with gallium nitride, Sci. Rep. 6 (2016) 22504.
[54] T. Nozaki, K. Hayashi, T. Kajitani, Thermoelectric properties of delafossite-type oxide $CuFe_{1-x}Ni_xO_2$ ($0 \leq x \leq 0.05$), J. Chem. Eng. Jpn. 40 (2007) 1205 1209.
[55] C. Ruttanapun, S. Maensiri, Effects of spin entropy and lattice strain from mixed-trivalent $Fe^{3+}/Cr^{3+}$ on the electronic, thermoelectric and optical properties of delafossite $CuFe_{1-x}Cr_xO_2$ ( x 0.25, 0.5, 0.75), J. Phys. D Appl. Phys. 48 (2015) 495103.
[56] P. Combis, P. Cormont, L. Gallais, D. Hebert, L. Robin, J.L. Rullier, Evaluation of the fused silica thermal conductivity by comparing infrared thermometry measurements with two-dimensional simulations, Appl. Phys. Lett. 101 (2012) 211908.